

University of Toronto

# Charge-to-mass ratio for the electron

Amir Koutahi, Enxi Huang

PHY294  
April 18, 2026

## Abstract

The charge-to-mass ratio of the electron was measured by observing the circular motion of an electron beam in the magnetic field produced by Helmholtz coils. Electrons accelerated through a known potential difference formed visible circular trajectories in a low-pressure gas tube. The beam diameters were measured using a self-illuminated scale and reflector to eliminate parallax. Because the scale was positioned 2.0 cm in front of the beam, this offset was added to all diameter measurements, with an estimated measurement uncertainty of  $\pm 0.1$  cm. Linearized theoretical relations were used to analyze data collected at constant voltage and constant current. From the linear fits, the external magnetic field and the charge-to-mass ratio were determined. The measured value,  $\frac{e}{m} = (1.7 \pm 0.2) \times 10^{11} \text{ C kg}^{-1}$ , is in reasonable agreement with the accepted value,  $1.7588 \times 10^{11} \text{ C kg}^{-1}$ , within experimental uncertainty.

## Contents

|          |   |          |
|----------|---|----------|
| <b>1</b> | <b>Introduction</b>                               | <b>1</b> |
| <b>2</b> | <b>Materials and Methods</b>                      | <b>1</b> |
| 2.1      | Materials . . . . .                               | 1        |
| 2.2      | Methods . . . . .                                 | 2        |
| <b>3</b> | <b>Data and Analysis</b>                          | <b>3</b> |
| <b>4</b> | <b>Discussion</b>                                 | <b>5</b> |
| <b>A</b> | <b>Uncertainty Propagation</b>                    | <b>6</b> |
| A.1      | Uncertainty in the Orbit Radius . . . . .         | 6        |
| A.2      | Uncertainty in the Curvature . . . . .            | 6        |
| A.3      | Uncertainty in the Charge-to-Mass Ratio . . . . . | 7        |
| A.4      | Off-axis Field Correction . . . . .               | 8        |

## 1 Introduction

In this experiment we determine the charge-to-mass ratio  $e/m$  of the electron by studying the motion of an electron beam in a magnetic field. A particle with charge  $e$  and mass  $m$  moving with velocity  $\mathbf{v}$  in a magnetic field  $\mathbf{B}$  experiences the Lorentz force

$$\mathbf{F} = e \mathbf{v} \times \mathbf{B}. \quad (1)$$

When  $\mathbf{v}$  is perpendicular to  $\mathbf{B}$ , the magnetic force acts as a centripetal force and the electron follows a circular path of radius  $r$ :

$$evB = \frac{mv^2}{r}, \quad (2)$$

where  $v$  is the electron speed.

The electrons are accelerated through a potential difference  $\Delta V$ , gaining kinetic energy

$$e\Delta V = \frac{1}{2}mv^2, \quad (3)$$

where  $\Delta V$  is the accelerating voltage. Combining Equations (2) and (3) gives

$$\frac{1}{r} = \sqrt{\frac{e}{2m}} \frac{B}{\sqrt{\Delta V}}. \quad (4)$$

In the apparatus, the magnetic field  $B$  is produced by Helmholtz coils carrying current  $I$ , together with a small external magnetic field  $B_e$ . By measuring the radius  $r$  for known values of  $\Delta V$  and  $I$ , we determine  $e/m$  and estimate the contribution of the external field.

## 2 Materials and Methods

### 2.1 Materials

The following equipment was used:

- Electron gun mounted inside low-pressure hydrogen glass bulb
- Pair of Helmholtz coils (radius  $R$ ,  $n$  turns per coil)
- DC power supply for coils (0–10 V)
- Variable accelerating voltage supply (0–300 V)
- 6.3 V filament power supply
- Digital voltmeter for anode voltage (resolution  $\pm 1$  V)
- Digital ammeter for coil current (resolution  $\pm 0.01$  A)
- Rheostat for current adjustment
- Self-illuminated scale and plastic reflector (for radius measurement)
- Connecting leads and power box

Measured quantities:

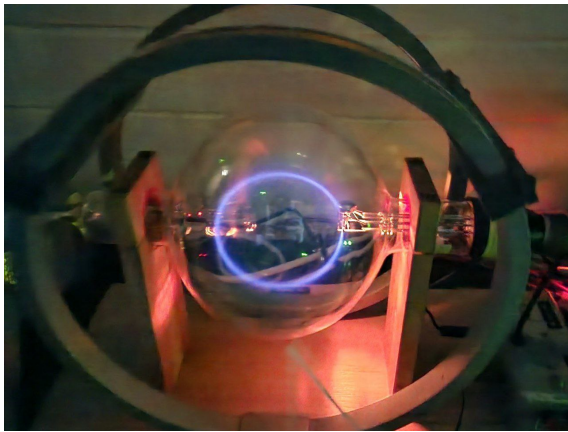
$$\Delta V = \text{accelerating voltage}, \quad I = \text{coil current}, \quad r = \text{electron orbit radius}.$$

## 2.2 Methods

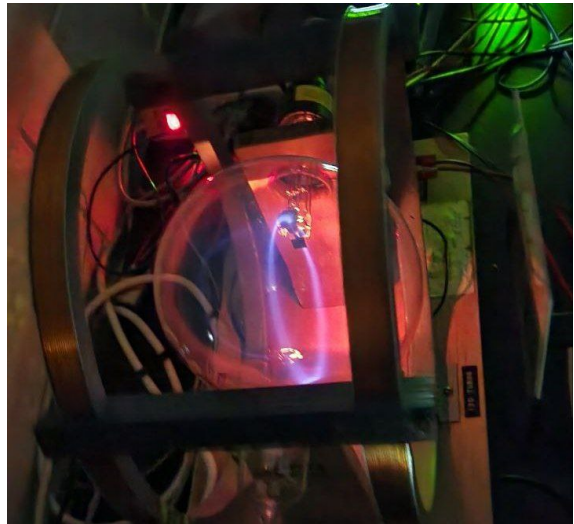
The glass bulb containing the electron gun was positioned at the center of the Helmholtz coils. The filament supply was turned on and allowed to heat for approximately 30 s before applying the accelerating voltage. The anode voltage  $\Delta V$  was then applied to produce a visible electron beam.

The current  $I$  through the Helmholtz coils was adjusted using the rheostat to generate a magnetic field perpendicular to the electron velocity. The polarity was adjusted if necessary to ensure a closed circular trajectory rather than a helical path.

Photographs of the electron beam were taken during the alignment stage to verify that the trajectory was approximately circular rather than helical. A front view and an oblique view taken at approximately  $45^\circ$  were used to confirm that the beam path remained circular from different viewing angles. This visual check helped ensure that the electron velocity was nearly perpendicular to the magnetic field before radius measurements were recorded.



(a) Front view of the electron beam pathway.



(b) Oblique view of the beam pathway at approximately  $45^\circ$ .

Figure 1: Photographs of the electron beam during alignment. The apparatus was adjusted so that the trajectory was as circular as possible rather than helical.

The radius  $r$  of the electron orbit was measured using the self-illuminated scale and plastic reflector to minimize parallax error. The scale was placed in front of the beam and viewed together with its reflected image in the plastic reflector. When the beam and its reflection coincided with the same scale marking, the observer's line of sight was effectively perpendicular to the measurement plane, thereby eliminating parallax. Two data sets were collected:

- Constant  $\Delta V$  with varying  $I$
- Constant  $I$  with varying  $\Delta V$

For each setting, the values of  $\Delta V$ ,  $I$ , and  $r$  were recorded along with their uncertainties. Care was taken to perform measurements promptly to reduce voltmeter drift.

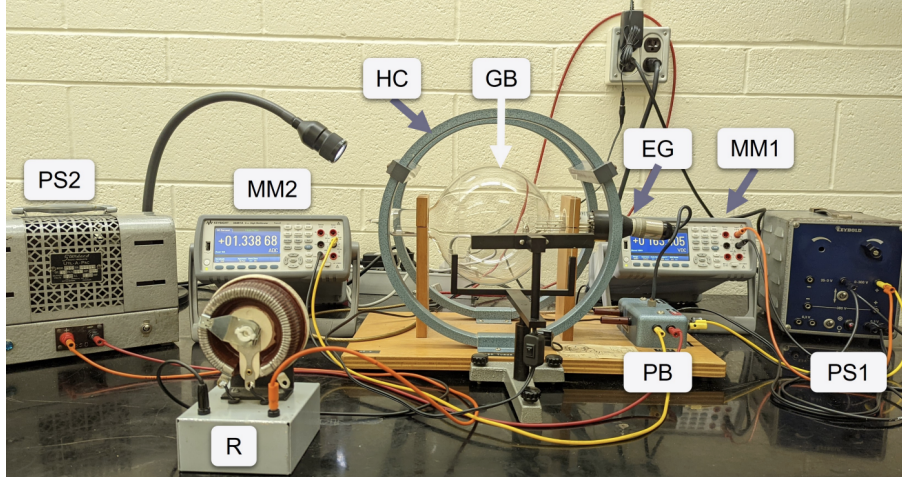


Figure 2: Experimental setup for the charge-to-mass ratio measurement. The glass bulb containing the electron beam is positioned between Helmholtz coils. The accelerating voltage supply, filament supply, and coil current supply are connected through the power box.

### 3 Data and Analysis

The uncertainty in the diameter measurement was estimated to be  $u_D = 0.1$  cm, which propagates to a radius uncertainty  $u_r = 0.05$  cm.

For the constant-voltage data set, the accelerating voltage was fixed at  $\Delta V = 200$  V. Equation (4) predicts a linear relation between the curvature and the magnetic field:

$$\frac{1}{r} = \sqrt{\frac{e}{2m}} \frac{1}{\sqrt{\Delta V}} (B_c + B_e)$$

Since the magnetic field produced by the Helmholtz coils is proportional to the current,  $B_c \propto I$ , the relation becomes

$$\frac{1}{r} = aI + b.$$

A weighted linear regression was therefore performed for  $1/r$  versus the coil current  $I$ . The fit produced a slope of  $(18.1 \pm 0.7) \text{ m}^{-1} \text{ A}^{-1}$  and an intercept of  $(0.7 \pm 0.9) \text{ m}^{-1}$ .

The goodness-of-fit statistics were  $R^2 = 0.9906$  and  $\chi^2_\nu = 1.7$ . These values indicate that the linear model provides an excellent description of the experimental data. The residuals were randomly distributed around zero with no systematic trend. Because the residuals are well spread and the value of  $R^2$  is very close to 1, the linear model provides a good description of the experimental data.

To estimate the extra magnetic field not produced by the coils, Equation (4) may be rewritten in the form

$$B = (B_c + B_e) = \sqrt{\frac{2m}{e}} \Delta V \frac{1}{r},$$

so that

$$B_c = \alpha \frac{1}{r} - B_e, \quad \alpha = \sqrt{\frac{2m}{e}} \Delta V.$$

In this form, a plot of  $B_c$  versus  $1/r$  is linear and the intercept corresponds to  $-B_e$ . In the present analysis, the intercept of the fitted linear relation indicates that  $B_e$  is on the order

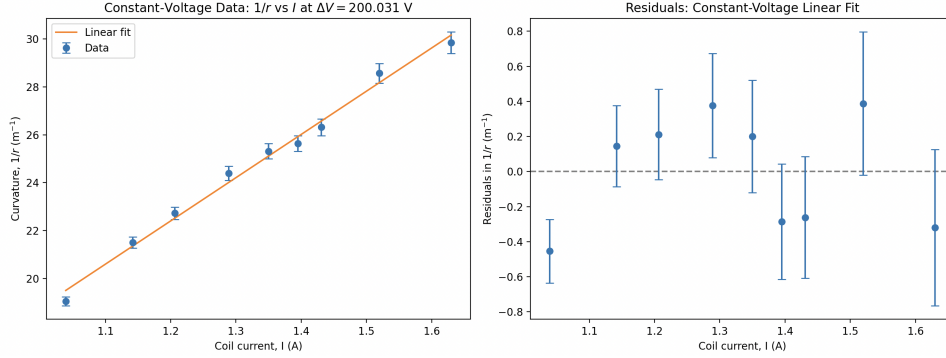


Figure 3: Linear fit of the curvature  $1/r$  as a function of coil current  $I$  for the constant-voltage data set ( $\Delta V = 200$  V).

of a few microtesla. This is smaller than the typical magnitude of the Earth’s magnetic field because only the component along the coil axis contributes to the measurement.

For the constant-current data set, the coil current was fixed at  $I = 1.04$  A. Equation (9) predicts

$$\frac{1}{r} = \sqrt{\frac{e}{m}} \frac{kI + \frac{1}{\sqrt{2}}I_0}{\sqrt{\Delta V}},$$

which implies a linear dependence between  $1/r$  and  $1/\sqrt{\Delta V}$ . A weighted linear regression of  $1/r$  versus  $1/\sqrt{\Delta V}$  was therefore performed.

The fit produced a slope of  $(4.5 \pm 0.3) \times 10^2 \text{ m}^{-1}\text{V}^{1/2}$  and an intercept of  $(-1.3 \pm 0.2) \times 10^1 \text{ m}^{-1}$ .

The goodness-of-fit statistics were  $R^2 = 0.9751$  and  $\chi^2_\nu = 2.2$ . These results demonstrate that the predicted linear dependence is reasonably well satisfied within experimental uncertainty. The residuals show no significant systematic pattern and are well distributed around zero. Together with the high  $R^2$  value, this indicates that the linear relation predicted by the theoretical model is consistent with the experimental data.

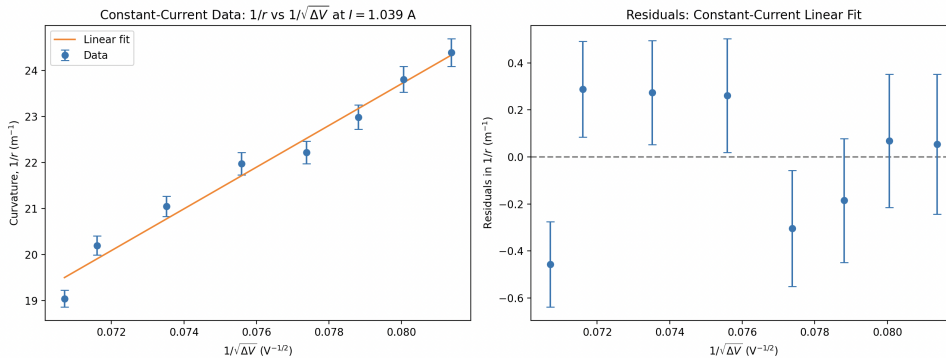


Figure 4: Linear fit of the curvature  $1/r$  as a function of  $1/\sqrt{\Delta V}$  for the constant-current data set ( $I = 1.04$  A). The linear behaviour confirms the theoretical prediction derived from Equation (9). Residuals show no significant systematic deviation.

Using Equations (9) and (10), together with the estimate of the external field  $B_e$ , the charge-to-mass ratio of the electron was obtained from the fitted slope. The experimen-

tally obtained value was found to be

$$\frac{e}{m} = (1.7 \pm 0.2) \times 10^{11} \text{ C kg}^{-1}.$$

The accepted value is

$$\frac{e}{m} = 1.7588 \times 10^{11} \text{ C kg}^{-1}.$$

Thus the measured value is consistent with the accepted value within experimental uncertainty.

## 4 Discussion

At low accelerating voltages and high coil currents the electron trajectory occasionally deviated from a perfect circular path. This occurs because the magnetic field produced by the Helmholtz coils is only perfectly uniform near the central axis. As the electron orbit moves farther away from the axis, the magnetic field decreases slightly. Consequently, different portions of the trajectory experience slightly different magnetic field strengths.

Therefore, not all parts of the trajectory are equally affected. The sections of the orbit farther from the coil axis are influenced more strongly, leading to small distortions from an ideal circle.

This effect introduces a systematic error in the measurement of the orbit radius. If the trajectory deviates from a circle, the measured diameter may not accurately represent the true radius used in the theoretical model. The error can be reduced by carefully adjusting the orientation of the tube so that the orbit remains centered and circular, and by avoiding extremely large radii where the field nonuniformity becomes more significant.

A more quantitative description of this effect is obtained by considering the off-axis dependence of the magnetic field. For off-axis distances  $\rho < 0.2R$ , the axial field differs from the on-axis value by less than 0.075%. For  $0.2R < \rho < 0.5R$ , the ratio is approximately

$$\frac{B(\rho)}{B(0)} = 1 - \frac{\rho^4}{R^4} \left( 0.6583 + 0.29 \frac{\rho^2}{R^2} \right)^2.$$

Because the electron beam is emitted from a fixed point, the circular orbit is not centered exactly on the coil axis, so  $\rho$  varies around the trajectory. As an approximation for large radii, the measured orbit radius may be used as a characteristic value of  $\rho$ . This correction helps explain why deviations from an ideal circular path are more noticeable at low  $\Delta V$  and high  $I$ , although it was not applied numerically in the present analysis.

Nearby magnetic materials and electronic devices may also influence the electron trajectory. Ferromagnetic objects can distort the local magnetic field by redirecting field lines, while electronic devices can produce additional magnetic fields. Bringing objects such as a cell phone near the apparatus can therefore slightly shift the electron beam path. Although these disturbances are typically small, they can still introduce measurable deviations in experiments where the magnetic field strength is on the order of tens of microtesla. In practice, this effect is not negligible if objects are brought very close to the bulb or coil region, and such objects should be kept away during measurement.

The measured external magnetic field was found to be on the order of a few microtesla, which is smaller than the typical magnitude of the Earth's magnetic field (approximately 25–65  $\mu\text{T}$ ). This difference is expected because the measurement detects only the component of the external field along the axis of the Helmholtz coils. Additionally, the

surrounding laboratory environment, including metallic structures and electrical equipment, may modify the effective background field. The uncertainty in  $B_e$  is governed mainly by the uncertainty in the intercept of the fitted linear relation, so it is relatively large compared with the small magnitude of the field itself.

Overall, the experimental results demonstrate that the circular motion of electrons in a magnetic field provides a reliable method for determining the charge-to-mass ratio of the electron. Despite several sources of systematic uncertainty, the measured value was in good agreement with the accepted value, confirming the validity of the theoretical model.

## A Uncertainty Propagation

### A.1 Uncertainty in the Orbit Radius

The electron orbit diameter  $D$  was measured directly using the illuminated scale. The true diameter was corrected for the 2.0 cm scale offset:

$$D_{\text{true}} = D_{\text{measured}} + 2.0 \text{ cm.}$$

The radius is therefore

$$r = \frac{D_{\text{true}}}{2}.$$

The measurement uncertainty of the diameter was estimated to be

$$u_D = 0.1 \text{ cm.}$$

Using standard uncertainty propagation,

$$u_r = \left| \frac{\partial r}{\partial D} \right| u_D$$

$$u_r = \frac{1}{2} u_D.$$

Thus

$$u_r = 0.05 \text{ cm.}$$

The reported radius measurements are therefore written as

$$r = r_{\text{measured}} \pm 0.05 \text{ cm.}$$

The uncertainty is reported with one significant digit, and the measured value is rounded to the same decimal place.

### A.2 Uncertainty in the Curvature

The curvature used in the analysis is

$$\frac{1}{r}.$$

Using propagation of uncertainty,

$$u_{1/r} = \left| \frac{d}{dr} \left( \frac{1}{r} \right) \right| u_r$$

$$u_{1/r} = \frac{u_r}{r^2}.$$

This uncertainty was used as the weighting factor in the linear regression.

### A.3 Uncertainty in the Charge-to-Mass Ratio

From the theoretical model,

$$\frac{\sqrt{\Delta V}}{r} = \sqrt{\frac{e}{m}} k \left( I + \frac{1}{\sqrt{2}} I_0 \right).$$

Rearranging gives

$$\sqrt{\frac{e}{m}} = \frac{s}{k},$$

where  $s$  is the slope obtained from the linear fit.

Therefore,

$$\frac{e}{m} = \left( \frac{s}{k} \right)^2.$$

Because  $e/m$  depends on the square of the slope, the uncertainty propagation gives

$$u_{e/m} = \left| \frac{d}{ds} \left( \frac{s^2}{k^2} \right) \right| u_s.$$

Thus

$$u_{e/m} = 2 \left( \frac{s}{k} \right) \frac{u_s}{k}.$$

Equivalently,

$$\frac{u_{e/m}}{e/m} = 2 \frac{u_s}{s}.$$

Using the fitted slope

$$s = (4.5 \pm 0.3) \times 10^2 \text{ m}^{-1} \text{ V}^{1/2},$$

the fractional uncertainty becomes

$$\frac{u_s}{s} \approx 0.07.$$

Therefore

$$\frac{u_{e/m}}{e/m} \approx 0.1.$$

This corresponds to an uncertainty of approximately 10%.

The final result is therefore reported as

$$\frac{e}{m} = (1.7 \pm 0.2) \times 10^{11} \text{ C kg}^{-1}.$$

The uncertainty is expressed with one significant digit and the measured value is rounded to the same decimal place, ensuring consistent significant figures.

#### A.4 Off-axis Field Correction

The magnetic field generated by the Helmholtz coils is nearly uniform only close to the central axis. For radial distances  $\rho$  smaller than  $0.2R$ , the axial field differs from the on-axis field by less than 0.075%. For  $0.2R < \rho < 0.5R$ , the field ratio is approximately

$$\frac{B(\rho)}{B(0)} = 1 - \frac{\rho^4}{R^4} \left( 0.6583 + 0.29 \frac{\rho^2}{R^2} \right)^2.$$

Because the electron beam is emitted from a fixed location, the orbit is not centered exactly on the axis, so  $\rho$  changes along the trajectory. For large orbits, a reasonable approximation is to take  $\rho \approx r$  when estimating the magnitude of the off-axis correction. This effect was considered qualitatively when interpreting deviations from ideal circular motion, but it was not applied numerically to the fitted data.